ON THE FINE STRUCTURE IN SPECTRAL BEHAVIOR AND ALTITUDE PROFILES OF THE OPTO–MICROPHYSICAL CHARACTERISTICS OF STRATOSPHERIC AEROSOL

R.F. Rakhimov

Institute of Atmospheric Optics,
Siberian Branch of the Russian Academy of Sciences, Tomsk
Received January 15, 1992

Results of the model estimates of the variability of opto–microphysical characteristics of the stratospheric aerosol in the process of eddy mixing and gravitational sedimentation of an eruptive cloud are discussed. The possible fine spectral structure in backscattering coefficient and lidar ratio variations are analyzed. Estimates show that spectral values of lidar ratio in the interval 30–40 nm about the wavelength $\lambda = 1.06$ *can change by 200–400% when the process of monodispersity of the coarse fraction culminates.*

As is well known, the mechanism of regeneration of the stratospheric aerosol assumes a long–period process of global scale in which not only lower tropospheric and upper mesospheric layers but also volcanogenic regions of an underlying surface are involved. Long–term and large–scale observations of the aerosol evolution in the atmosphere up to the altitudes of 30–40 km and higher are necessary to predict the variability of the layer state and seems to be possible only using the means of laser detection and ranging. However, in this case the conservative impurity hypothesis, which usually provides the basis for the inversion of lidar measurements, appears to be obviously insufficient. Data on the behavior of optical–radar parameters at various sections of the radiation spectrum as functions of not only altitude but also time are needed.

The peculiarity of evolution of aerosol anomalies in the stratosphere is also caused by the noticeable altitude variation in the density and viscosity of air[1] (it is valid, to a greater degree, for the mesosphere). Sedimentation and diffusion spreading whose intensity depends on the above–indicated factors are of primary importance in the process of disappearance of the observed aerosol formations.

The technique of reductive numerical modeling of the opto–microphysical parameters of the stratospheric aerosol was previously presented in Ref. 1. It was noted among the other results that at certain stages of the examined process quite an unexpected effect could appear, namely, the narrowing of the width of the distribution mode due to the increase in the sedimentation efficiency of larger particles (the effect of local monodispersity).

In this paper the given tendency is analyzed in more detail. The system of equations for the integral parameters provided in Ref. 2 the initial mathematical basis for the model description of the transformation of the structure of the eruptive cloud. Let us write this system in the form of the system of equations for the components of the parameter vectors $\hat{Q}_i = \{N_i, S_i, V_i\}$ which characterize the particle size spectrum of aerosols in the ith fraction in terms of the lognormal distribution

$$\frac{\partial \hat{Q}_i(z, t)}{\partial t} = \frac{\partial}{\partial z} D(z) \frac{\partial \hat{Q}_i(z, t)}{\partial z} - \frac{\partial}{\partial z} [W_{qi}(z, t)\, \hat{Q}_i(z, t)],$$

where the parameter vector $\hat{Q}_i(t, z)$ means individually either the total volume V_i or the cumulative cross section S_i or simply the number density N_i of aerosols at the given point with the coordinate z; t is the running time of the process, W_{qi} is the average rate of the Stokes sedimentation of particles in the ith fraction estimated for each equation from the modal radius of the probability density function of the corresponding integral parameter distribution over the size spectrum. The coefficient of eddy diffusion $D(z, t)$, according to Ref. 3, depends weakly on the altitude in the lower and middle stratosphere. Taking the seasonal trends into account, its values change from 0.01 to 1.0 m^2/s. In addition, the typical altitude range of location of volcanogenic aerosol layers coincides with that of minimum intensity of eddy mixing.[4] In the Junge stratospheric layer the wind averaged over long–time intervals is negligible and may be set equal to zero in this consideration. In the model only the rate of the Stokes sedimentation of the particles is taken into account, which is given by the formula

$$W_{qi} = \frac{2g\rho R_{qi}^2}{9\eta} (1 + C_{Khi}\,\mathrm{Kn}),$$

where R_{qi} is the particle radius, g is the acceleration of gravity, ρ is the density of aerosol substance, η is the dynamic viscosity of air, $\mathrm{Kn} = l/R$ is the Knudsen constant, l is the mean free path length for air molecules, and C_{Chi} is the Cunningham adjustment factor averaged over the particle size spectrum in the i th fraction, which is given by the formula

$$C_{Chi} = 1.257 + 0.40 \exp(-0.55/\mathrm{Kn}).$$

Assuming that the mean free path length for air molecules varies according to the barometric law with the temperature T being independent of altitude, we may use the following generalization for the vertical sedimentation rate of particles W:

$$W = -\frac{2g\rho R_{qi}^2}{9\eta} - \frac{2g\rho R}{9\eta} C_{Chi} l_0 \exp\left(\frac{mgz}{k_B T}\right) = -A - B\exp(\gamma z),$$

0235-6880/92/05 337-07 $02.00

where m is the mass of air molecules, K_B is Boltzmann's constant, T is the average temperature of the layer; l_0 is the mean free path length of molecules under normal conditions.

In modeling the evolution of the eruptive cloud composition the same altitude range h = 12–29 km was considered. However, the certain changes compared to Ref. 1 were introduced in the choice of the values of the parameters determining the conditions of the evolution. Thus, in particular, in order to avoid the side effects of mixing of the size spectra of injected and background aerosols the altitude variation of the integral parameters of the latter $\hat{Q}_i^{bg} = \{N_i^{bg}, S_i^{bg}, V_i^{bg}\}$ was stylized following, on the whole, the exponential dependence

$$\hat{Q}_i^{bg}(z) = \hat{Q}_{i0}^{bg} \exp\{-\hat{G}_{qi}^{bg}(z - 12)\},$$

where $\hat{Q}_{i0}^{bg}$ are the values of the integral parameters of the background component at the altitude z = 12 km and $\hat{G}_{qi}^{bg}$ is the parameter vector assigning the vertical gradients of the corresponding integral parameters of the background component. The specific values of $\hat{Q}_i^{bg}$ and $\hat{G}_{qi}^{bg}$ are given in Table I.

TABLE I.

Fraction	N_{i0}^{bg}	G_{ni}^{bg}	S_{i0}^{bg}	G_{si}^{bg}	V_{i0}^{bg}	G_{vi}^{bg}
Accumulative	3.0e–0	0.190	5.0e–1	0.205	1.2e–2	0.226
Coarsely disperse	4.6e–3	0.205	2.0e–1	0.266	2.4e–1	0.276

The adjustment factors were also introduced for the layer temperature T = 217°C, air viscosity $\eta = 1.42 \cdot 10^{-5}$ N·s/m^2, mean free path length of molecules $l_0 = 6.3 \cdot 10^{-8}$ m, and density of aerosol substance $\rho = 1.5 \cdot 10^3$ kg/m^3. The choice of ρ was caused by predominating sulphur compounds in the stratospheric aerosol composition.

The disperse structure of aerosols predicted within the framework of the proposed model was estimated in terms of the integral parameters; in addition, the structure fractional parametric model of the form[3]

$$f(R) = \frac{dN}{dR} = AR^{-3} \sum_i^k M_i \exp\{-b_i[\ln(R/R_i)]^2\} \qquad (1)$$

was used as the approximation model. The well–known lognormal distribution was the prototype of the elements of this model. Essentially, the value of the parameter b_i was inversely proportional to the square of the standard deviation $b_i = 0.5\sigma^{-2}$. The parameter $f_i = AM_i$ was used for graphical representation of data. The starting altitude of the eruptive emission of the coarsely dispersed fraction was assumed to be equal to 26 km and that of the accumulative fraction was 21 km.

The choice of D = 0.35 m^2/s was caused by the desire to show the possible monodispersity of coarse–particle aerosols even for more intensive mixing of air masses. The following initial values of the integral parameters of aerosols of the eruptive cloud for the accumulative fraction were chosen:

$N_{a0} = 1.37 \cdot 10^4$ cm^{-3}, $S_{a0} = 1.15 \cdot 10^3$ μm^2 cm^{-3}, and V_{a0} = 50.3 μm^3 cm^{-3};

those for the coarsely disperse fraction were: N_{c0} = 1.79 cm^{-3}, S_{c0} = 204 μm^2 cm^{-3}, V_{c0} = 281 μm^3 cm^{-3}.

Thus, corresponding parameters of the particle size spectrum for the accumulative fraction were: R_a = 0.11 μm, b_a = 1.58, and f_a = 64.8; for the coarsely disperse fraction they were: R_c = 3.7163 μm, b_c = 2.3716, and f_c = 14.1.

Calculations show that as a result of the polidisperse character of the initial composition of aerosols injected into the stratosphere, the noticeable mismatch occurs in the rates of evolution of the vertical structure of the integral parameters (Fig. 1 *a–c*). Despite the intense eddy mixing and a tendency to the vertical uniformity of the variation in the integral parameters of aerosols in the lower part of the eruptive cloud (Fig. 1 *a–c*), the size spectrum of the coarsely disperse fraction undergoes considerable altitude deformations (Fig. 2 *a–c*) and, in addition, reveals the irregularity of the variation in the parameters $f_2(z)$, $b_2(z)$, and $R_2(z)$.

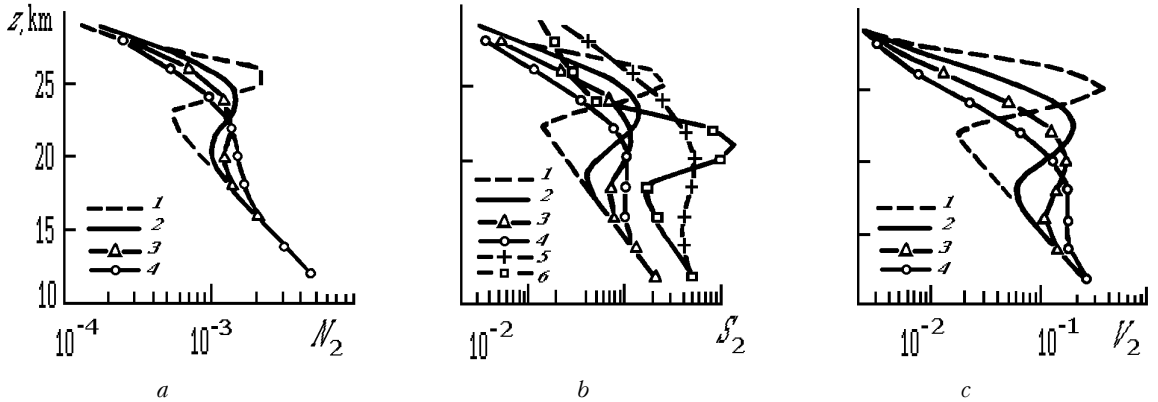

a *b* *c*

FIG. 1. Deformations of the vertical profiles of the integral parameters of the disperse structure of the coarse fraction: a) N_2, *b)* S_2, *and c)* V_2. *Curves 1–4 correspond to t* = 15, 65, 115, *and* 160 *days; curves 5 and 6 – to t* = 15 *and* 160 *days for* S_1.

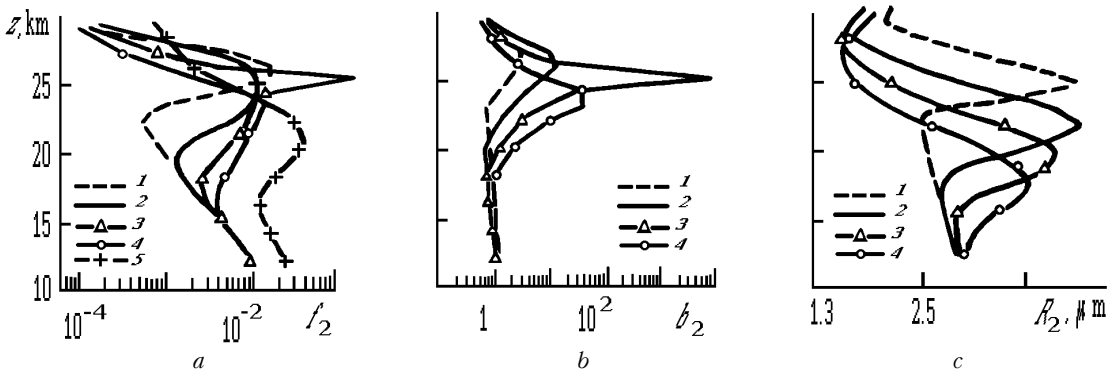

FIG. 2. Deformations of the vertical profiles of the parameters of distribution function (1) of the coarsely disperse fraction: a) f_2, b) b_2, and c) R_2 calculated from the data shown in Fig. 1 (designations are the same as in Fig. 1). Curve 5 is for accumulative fraction f for t = 115 days.

Quite complicated processes of mixing proceed in the plume of the eruptive cloud, that facilitate the formation (for a time) of the local anomaly of aerosols with very narrow size spectrum ($\sigma_2 \sim 0.004$). The peak value of the spectral parameter f_2 is also typical of this altitude. This parameter comprises generally the information about the behavior of the cumulative cross section of particles and on the width of the spectrum

$$f_2 = S_2/\sqrt{16\pi^3/b_2}\,,$$

and the existence of the local extremum in $f_2(z)$ at the altitude z = 25 km is entirely caused by the sharp narrowing of the size spectrum at this altitude, since the function $S_2(z)$ (Fig. 1 *b*, curve *3*) is quite smooth.

For the given intensity of eddy mixing the Stokes sedimentation rate for the accumulative fraction is insufficient for any ordering processes in the disperse structure analogous to the local monodispersity of the coarsely disperse fraction. The vertical profile $f_1(z)$ (curve *5*) for t = 115 days is shown in Fig.2 for comparison.

As a result of the intense sedimentation of the largest particles of the coarsely disperse fraction their characteristic radius at the center of the cloud (estimated from the volume number density of particles) is steadily decreasing, as can be seen from the results in Fig. 2c.

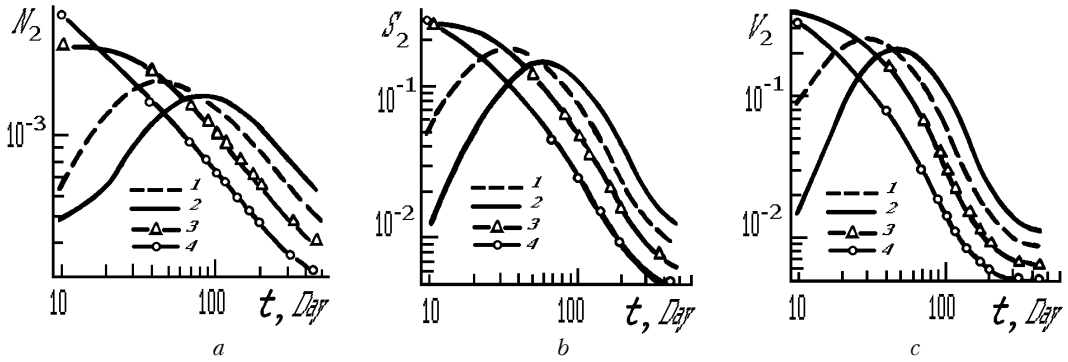

FIG. 3. Variation in the integral parameters of the disperse structure of the coarse fraction vs time: a) N_2, b) S_2, and c) V_2. Curves 1–4 correspond to z = 23, 24, 25, and 26 km.

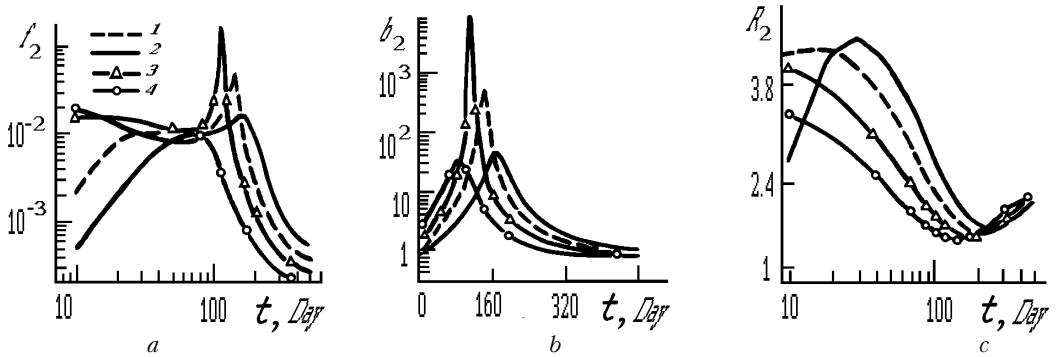

FIG. 4. Variation in the parameters of size spectrum (1) of the coarsely disperse fraction vs time: a) f_2, b) b_2, and c) R_2. Curves 1–4 correspond to z = 23, 24, 25, and 26 km.

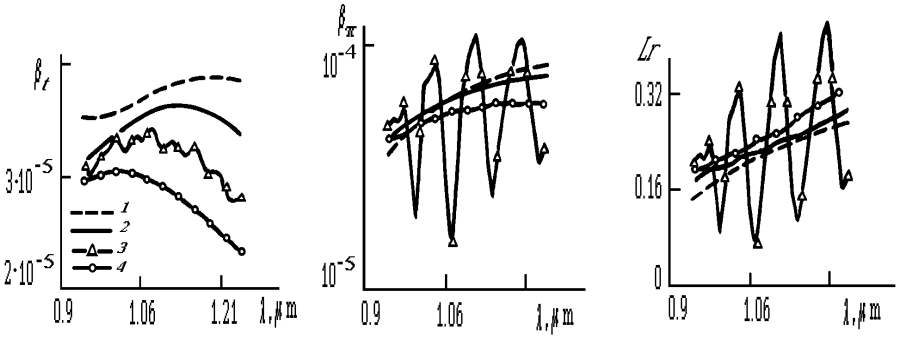

FIG. 5. Spectral behavior of aerosol light scattering parameters: a) extinction coefficient β_ε (km^{-1}), *b) volume coefficient of backscattering* β_π (km^{-1}), *and c) lidar ratio Lr at an altitude of* 25 *km. Curves 1–4 correspond to t =* 95, 105, 115, *and* 125 *days.*

If the results in Fig. 3 *a–c* show the consequences of eddy mixing and gravitational sedimentation which are quite predictable for integral parameters of the eruptive cloud, then the parameters of particle size spectrum (1) (Fig. 4 *a–c*) are subject to much more complicated variations. Though the monodispersity process culminates within the 24–25 km altitude range for t = 116.5 days and the particle size spectrum at altitudes outside of the indicated range gets narrower, but insufficiently for revealing the fine structure in the spectral behavior of the optical parameters (Fig. 5). Then, as the degradation of the number density of aerosol substance occurs the spreading of the spectrum and its broadening up to the background level take place.

Nonuniformity and instability of the disperse structure of stratospheric aerosols are combined with the variety of chemical compounds determining their physicochemical composition. Thus, for example, the measurements performed in Ref. 4 just after volcanic eruptions showed a large number of silicate particles. It was noted in a number of measurements the manifestation of the fragments and combustion products of meteor dust. The question about the compound being dominant in the stratospheric aerosol composition: ammonium sulphate, persuphate or sulphuric acid, has still not answered. In particular, according to data of Ref. 6 the content of ammonium sulphate is increased at altitudes above 20 km. The hypothesis that aerosols have the concentrically nonuniform dielectric structure was approved in estimating the light scattering properties of the eruptive cloud. Data on the spectral behavior of the complex refractive index (CRI) of ammonium sulphate were used as optical constants of the particle core whose coating was assumed to consist of sulphuric acid.

Calculations of the spectral variability of the light scattering parameters of stratospheric aerosols about the lidar wavelength λ = 1.06 μm are shown in Fig. 5 *a–c*. The revealed tendency of the local monodispersity leads to the appearance of the fine spectral structure in the behavior (vs the wavelength) of not only the extinction coefficient β_ε (Fig. 5 *a*) but, first of all, of the backscattering coefficient β_π and of the lidar ratio $Lr = \beta_\pi/\beta_\varepsilon$ (Fig. 5 *c*). The fine spectral structure in the behaviour of the above–indicated characteristics is caused by the narrowing of the size spectrum width of the coarsely disperse fraction so much that it lies within the limits of a single peak in the curve of the backscattering efficiency Q_{bs} ($\rho = 2\pi R/\lambda$) (Fig. 6 *a* and *c*). When the wavelength increases, in fact, we can trace the behavior of the curve of extinction and backscattering efficiencies.

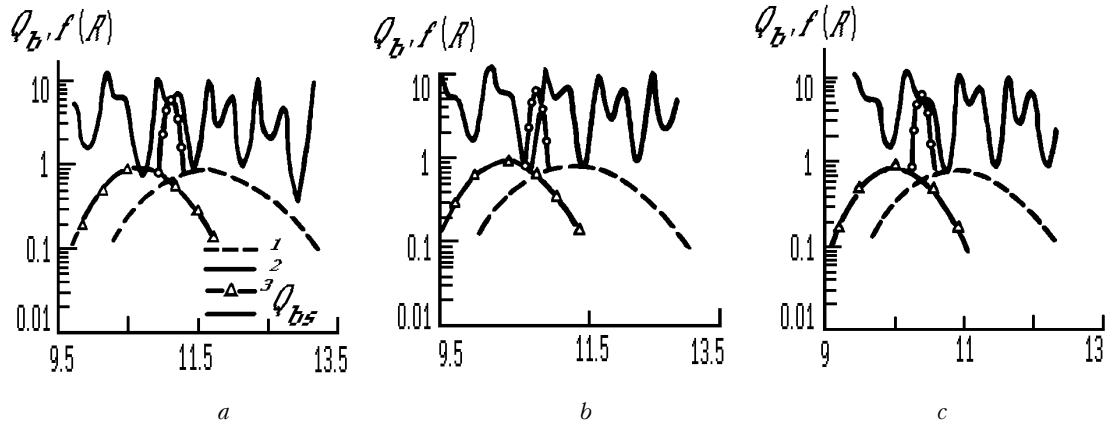

a *b* *c*

FIG. 6. The position of the particle size spectrum of the coarsely disperse fraction with respect to the curve of backscattering efficiency $Q_{bs}(\rho = 2\pi R/\lambda)$: *a)* λ = 1.03 μm, *b)* λ = 1.06 μm, *and c)* λ = 1.10 μm. *Curves 1–3 are the spectra calculated for t =* 105, 115, *and* 125 *days, respectively; curve* 4 *denotes* Q_{bs}.

The last circumstance can be applied to indicate the dielectric properties of the particle substance. At the same time, calculations show that one should be careful in interpreting the sounding data in order to avoid the erroneous identification of the fictitious layers with the increased particle number density as a result of neglecting the complicated spectral behavior of the lidar ratio when lidar data are inverted based on the single–frequency equation of laser sensing.[3]

Data on the temporal variability of the optical–radar parameters of the stratospheric aerosols being discussed within the 23–26 km altitude range for three wavelengths $\lambda = 1.02$, 1.06, and 1.10 μm are shown in Figs. 7 and 8 *a–c*. They show that the fine structure in the spectral behavior of the optical–radar characteristics of the layers with anomalously narrow spectrum is relatively short–lived. In addition, the lidar ratio variations can be opposite in sign at neighboring wavelengths. Identifying the effect under discussion would call for obtaining detailed temporal and altitude behaviors of the measurable parameters with the use of the sources operating at neighboring wavelengths with $\Delta\lambda = 20–40$ nm.

The analysis of the temporal variability in the optical–radar characteristics shows that at first the volume backscattering coefficient at the center of the cloud decreases quite sharply, but then for a time the rate of its decay is slowed down and it can even start to increase again at some altitudes, and only after the lapse of six months the decrease of β_π acquires stable exponential character (Fig. 7 *a–c*).

The time interval $t = 95–125$ days which is analyzed in Fig. 5 is shorten deliberately in order to follow the transformation of the spectral behavior of optical parameters at that very stage when the size spectrum starts to differ strongly from the background one. In particular, the noticeable qualitative change in the behavior of $\beta_\varepsilon(\lambda)$ is explained by this very circumstance that predetermines the significant variation of the lidar ratio (Fig. 8 *a–c*) despite the behavior of $\beta_\pi(t)$ differs insignificantly for neighboring wavelengths in Fig. 7 *a–c* (except the vicinity of $t = 116.5$ days).

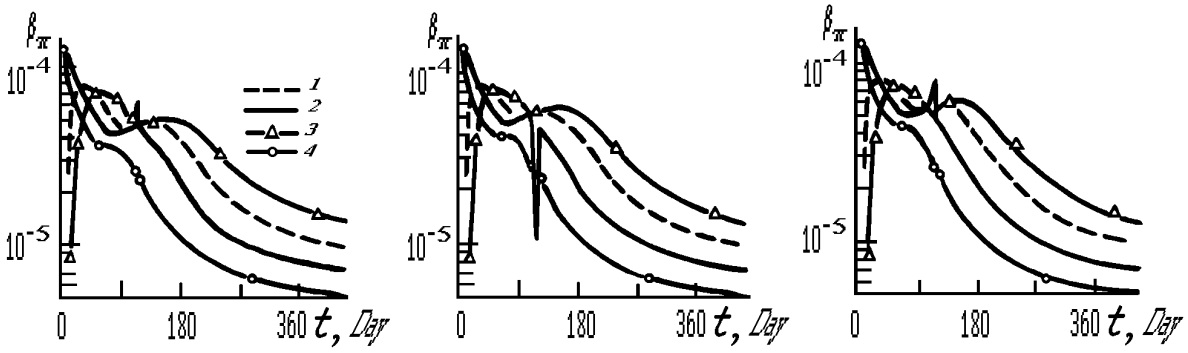

a *b* *c*

FIG. 7. Variation in the volume backscattering coefficient β_π (km^{-1}) vs *time: a)* $\lambda = 1.02$ μm, *b)* $\lambda = 1.06$ μm, *and c)* $\lambda = 1.10$ μm. *Curves 1–4 correspond to* $z = 23$, 24, 25, *and* 26 *km.*

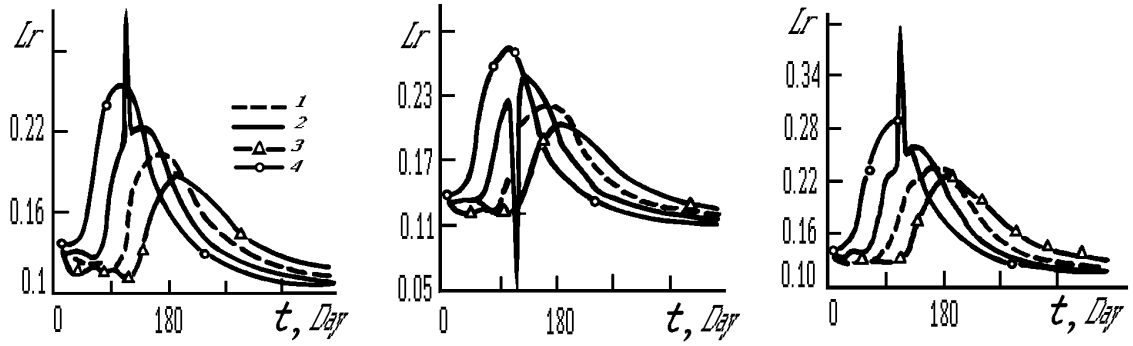

a *b* *c*

FIG. 8. Variation in the lidar ratio L_r vs *time: a)* $\lambda = 1.02$ μm, *b)* $\lambda = 1.06$ μm, *and c)* $\lambda = 1.10$ μm. *Curves 1–4 correspond to* $z = 23$, 24, 25, *and* 26 km.

Figure 9 *a* shows the comparison of model estimates with the field measurements performed after the eruption of the El–Chichon volcano. This comparison shows that the variations of the examined characteristics of the stratospheric cloud are qualitatively similar. At the same time, it should be noted that the use of the *a priori* lidar ratio for inverting the sounding data contradicts to its complicated altitude and temporal variations (Fig. 9 *b*).

The problem of transformation of the size spectrum of stratospheric aerosols is also actual from the viewpoint of estimating the efficiency of the increase in turbidity and the deformations of the scattering phase function in the stratosphere when the aerosol–forming compounds being additional to the background level are injected. The vertical profile of the mean cosine of the scattering phase function is shown in Fig. 9 *c* to illustrate the effect of

interfractional mixing. The given characteristic is often used to estimate the radiative effect of the eruptive cloud when solving the radiative transfer equation in a two–flow approximation.[3]

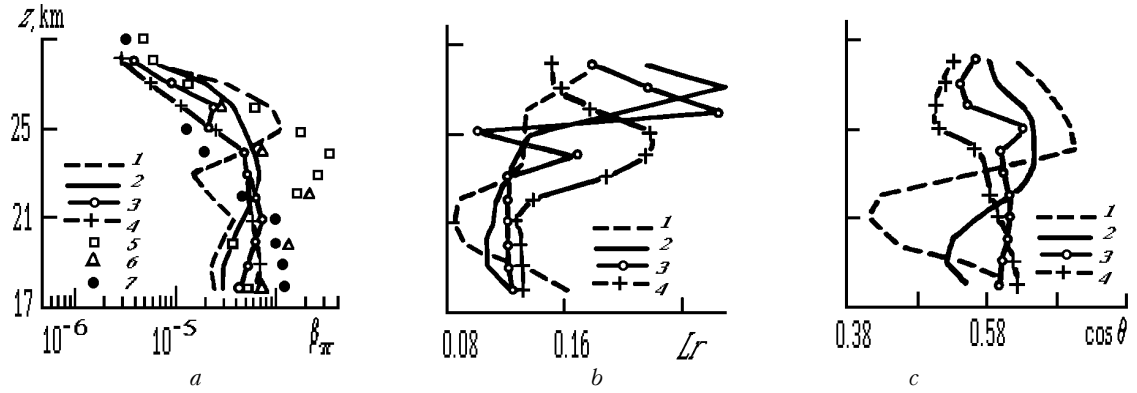

FIG. 9. Deformations of the vertical profiles of aerosol light scattering parameters: a) β_π (km^{-1}), *b) Lr, and c)* $\cos\theta$ *calculated from the data shown in Fig. 1 (designations are the same as in Fig. 1) in comparison with the data taken from Ref. 3 (curves 5–6).*

The sharp variations in the lidar ratio within the fixed altitude range (Fig. 9*c*) are also the result of the interfractional mixing of two local emissions having different starting altitudes (26 and 21 km) and different, as was noted previously, dispersion compositions. Taking into account the low intensity of eddy mixing within the layer, apparently, it should be admitted that such a sharp variation of optical parameters is a typical phenomenon at early stages of the postvolcanic relaxation of the stratospheric layer.

Evolution of the structure of the eruptive cloud and its gravitational stratification has been analyzed in this paper without taking into account the real physicochemical diversity of volcanogenic aerosols and the seasonal trends in the meteorological state of the layer. Polydispersity of stratospheric aerosols was assumed to be the main factor of the altitude transformation of their size spectrum. The chosen value $D = 0.35$ m^2 s^{-1} was considered to be season–averaged for the examined layer above 20 km (Ref. 3). In summer the efficiency of monodispersity increases for weak eddy mixing when $D \sim 100$ cm^2 s^{-1} and *vice versa*, in winter for increased intensity of eddy mixing within the layer under the impact of large–scale planetary waves when the diffusion coefficient reaches the values $D \sim 1$ m^2 s^{-1}, the efficiency of monodispersity of coarsely disperse aerosols with low specific density $\rho \sim 1$–3 g/cm^3 is low. However, for particles with higher specific density $\rho \sim 7 - 12$ g/cm^3 the monodispersity of the size spectrum is nevertheless possible for the above–indicated intensity of mixing, especially if the size spectrum of the emission is much more shifted toward the large particles.

The effect of local monodispersity predicted for the stratospheric layer as a result of model calculations was not found experimentally in the surface layer apparently due to intensive eddy mixing and dominating contribution of the submicron particles to backscattering that results in masking of the fine spectral structure of $\beta_\pi(\lambda)$. To confirm the possibility of this effect, the special–purpose laboratory experiment is required in which the atmospheric pressure and temperature should be decreased in the volume under study down to the values typical of the conditions of the stratosphere in order to increase the particle sedimentation rate.

REFERENCES

1. R.F. Rakhimov, Atm. Opt. **4**, No. 6, 474–479 (1991).
2. R.F. Rakhimov, Atm. Opt. **4**, No. 5, 389–394 (1991).
3. T. Shibata, M. Fujiwara, and M. Hirono, J Atmos. Terr. Phys. **46**, No. 12, 1121–1146 (1984).
4. O.B. Toon and J.M. Pollack, J. Appl. Met. **15**, No. 3, 225–246 (1976).
5. J.P. Shedlovsky and S. Paisley, Tellus **18**, 499–503 (1966).
6. E.K. Bigg, A. Ono, and W.J. Thompson, Tellus **22**, 550–563 (1970).
7. E.K. Bigg, J. Atmos. Sci. **32**, 910–917 (1975).
8. M. Hirono, et al., Geof. Int. **23–2**, 259–276 (1984).